Influence of the saddle-splay energy on the structure of cholesteric liquid crystals confined to a capillary

A. Kilian and A. Sonnet
Institut für Theoretische Physik, Technische Universität Berlin, D-10623 Berlin, Germany
(Received 10 May 1995)

We calculate the director field of a cholesteric liquid crystal confined to a capillary. It is assumed to be rotationally symmetric, defect free, and homogeneous along the capillary axis. The boundary coupling is either rigid or planar-free. We found that the saddle-splay energy induces a preferred direction for the director at the capillary wall. Thus this setup is suitable for high precision measurements of K_{24}. Since our result holds for capillaries of arbitrary radius, it is a counterexample to the standard argument that K_{24} can be neglected for geometries which are defect free and large enough.

PACS number(s): 61.30.Gd

I. INTRODUCTION

The saddle-splay term occurring in the Frank free energy has been known for decades [1]. In director field calculations it had usually been omitted. The standard argument was that it can be transformed into a surface term by Gauss's theorem, and is therefore of minor influence for large samples because, in this case, surface energies are small compared to bulk energies. Also, no experimental data for K_{24} were available.

During the last few years, the saddle-splay energy has attracted new interest [2–5]. It has been found that in submicrometer-sized cavities, the influence of K_{24} on the director configuration is crucial, and a number of measurements have been performed [2,6].

This paper presents a theoretical examination of a cholesteric liquid crystal confined to a capillary. The director field is assumed to be rotationally symmetric, defect free, and homogeneous along the capillary axis. The boundary coupling is either rigid or planar-free [7], which means that the director may freely rotate within the local tangent plane of the surface.

The free energy density of a cholesteric liquid crystal as a function of the director $\mathbf{n}$ is expressed as the sum of an elastic and a chiral contribution (when no external fields are present):

$$f = f_{el} + f_{chiral}, \tag{1}$$

where

$$f_{el} = \frac{K_1}{2}(\nabla\cdot\mathbf{n})^2 + \frac{K_2}{2}(\mathbf{n}\cdot\nabla\times\mathbf{n})^2 + \frac{K_3}{2}(\mathbf{n}\times\nabla\times\mathbf{n})^2 - \frac{K_{24}}{2}\nabla\cdot(\mathbf{n}\times\nabla\times\mathbf{n}+\mathbf{n}\nabla\cdot\mathbf{n}), \tag{2}$$

$$f_{chiral} = q_0 K_2 \mathbf{n}\cdot\nabla\times\mathbf{n}; \tag{3}$$

$q_0 = 2\pi/p_0$ is a measure for the helical twisting power, and p_0 is the intrinsic cholesteric pitch. For simplicity, we restrict our analysis to terms in the first derivative of the director. Therefore, in Eq. (2) we have neglected the splay-bend surface contribution $K_{13}\nabla\cdot(\mathbf{n}\nabla\cdot\mathbf{n})$. The K_{24} term, on the other hand, does not contain any second derivatives, as can be seen by an explicit calculation [8] [cf. also Eq. (4) below].

As an aside, when $K_1 = K_2 = K_3 = K_{24} =: K$, Eq. (2) simplifies to

$$f_{el}^{simple} = \frac{K}{2}(\nabla\mathbf{n})^2. \tag{4}$$

This implies that the so called one-constant approximation contains, in contrast to the usual splay-twist-bend ansatz, a saddle-splay contribution. There are cases where the inclusion of the K_{24} term is more essential than using exact values for K_1 and K_3. In other words, the one-constant approximation (4) may lead to more realistic results. The geometry considered below represents an example.

We look for director configurations that are rotationally symmetric, defect free, and homogeneous along the capillary axis. An appropriate ansatz is the double-twist configuration [9], which is already known as an example where the K_{24} term is of importance [10,11]. It has the specific form

$$\mathbf{n} = \begin{pmatrix} \sin\vartheta(r)\sin\phi \\ -\sin\vartheta(r)\cos\phi \\ \cos\vartheta(r) \end{pmatrix}, \tag{5}$$

where the capillary axis points in the z direction and (r,ϕ) are the radius and polar angle in cylindrical coordinates, i.e., $x = r\cos\phi$, $y = r\sin\phi$. In order to illustrate this ansatz by example, Fig. 1 depicts the director field Eq. (5) with a linearly growing $\vartheta(r)$. It should be mentioned that this particular choice does not correspond to a minimum energy, but it is very similar to some of the minimizing configurations we have computed.

The free energy density Eq. (2) of the director field Eq. (5) has the specific form

$$f = \frac{K_2}{8r^2}\left[\sin(2\vartheta) + 2r\vartheta' - 2rq_0\right]^2 - \frac{K_2}{2}{q_0}^2 + \frac{K_3}{2r^2}\sin^4(2\vartheta) - \frac{K_{24}}{2r}\vartheta'\sin(2\vartheta). \tag{6}$$

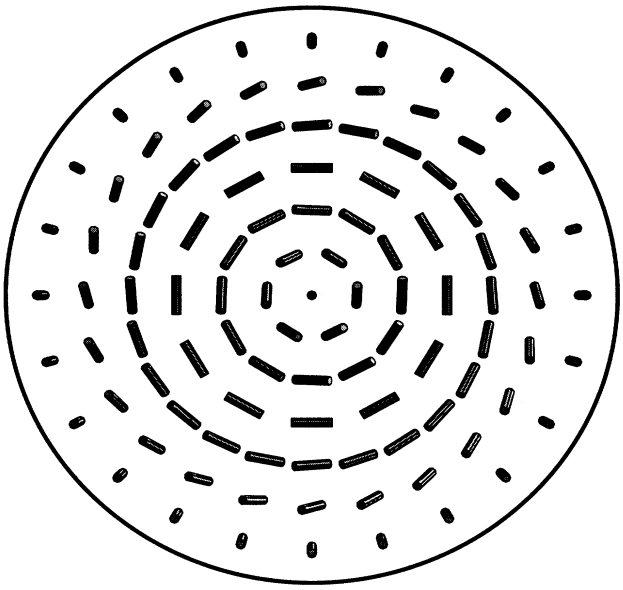

FIG. 1. Sample director field with $\vartheta(\hat{r}) = \pi\hat{r}$. Note that this is not an equilibrium director configuration, but it is quite similar to some of the computed solutions.

The dependence of ϑ on r has been omitted for brevity. Note that this configuration exhibits no splay, but a bend deformation that is maximal at sites where the director lies in the x-y plane.

From now on, all lengths will be expressed in units of the capillary radius r_{cap}, that is,

$$r \to \hat{r} r_{cap}, \quad q_0 \to \frac{\hat{q}_0}{r_{cap}}, \quad \frac{d}{dr} \to \frac{1}{r_{cap}} \frac{d}{d\hat{r}}, \quad \text{etc.} \tag{7}$$

This transformation leaves Eq. (6) unchanged, except that r and q_0 get a circumflex. The total energy (per unit length) is

$$F = \int_0^1 2\pi \hat{r} f d\hat{r}. \tag{8}$$

The total saddle-splay contribution (per unit length) depends only on the value of ϑ at the capillary wall, i.e.,

$$\begin{aligned} F_{saddle/splay} &= \int_0^1 2\pi \hat{r} f_{saddle/splay} d\hat{r} \\ &= \frac{\pi K_{24}}{2} \left[\cos 2\vartheta(1) - \cos 2\vartheta(0)\right], \end{aligned} \tag{9}$$

where $\vartheta(0) = 0$ is required by continuity of the director field in the center.

II. THE NUMERICAL ALGORITHM

In order to achieve a stationary director field, it is necessary that the variation δF of Eq. (8) vanish, i.e.,

$$\delta F = 2\pi \int_0^1 \left(\frac{\partial(\hat{r} f)}{\partial \vartheta} \delta\vartheta + \frac{\partial(\hat{r} f)}{\partial \vartheta'} \delta\vartheta' \right) d\hat{r} = 0. \tag{10}$$

Partial integration yields the Euler-Lagrange equations

$$\frac{\partial(\hat{r} f)}{\partial \vartheta} - \frac{\partial}{\partial \hat{r}} \frac{\partial(\hat{r} f)}{\partial \vartheta'} = 0 \tag{11}$$

for the bulk and

$$\left. \frac{\partial(\hat{r} f)}{\partial \vartheta'} \right|_{\hat{r}=1} = 0 \tag{12}$$

for the boundary (at $\hat{r} = 1$). Equation (12) is needed only when ϑ is not prescribed at the capillary wall, i.e., $\delta\vartheta \neq 0$. In this case, the director at $\hat{r} = 1$ is not entirely free but, rather, it is confined to the local tangent plane of the capillary; cf. Eq. (5). This type of boundary condition is referred to as "planar-free" [7]. Nonrubbed glass surfaces exhibit approximately such a coupling.

Only a few analytical solutions of Eq. (11) are available. For example, if $K_2 = K_3$, $q_0 = 0$, and $\vartheta(1) = \pi/2$, we have

$$\vartheta(\hat{r}) = 2 \arctan(\hat{r}), \tag{13}$$

and for $K_3 = q_0 = 0$ and $\vartheta(1) = \pi/4$, we have

$$\vartheta(\hat{r}) = \arctan(\hat{r}). \tag{14}$$

In order to solve Eq. (11) numerically for arbitrary values of K_1, K_2, K_3, and q_0, we developed the following successive over-relaxation algorithm on a uniform grid:

$$\vartheta^{new}(i) = (1 - \omega)\vartheta(i) + \omega\tilde{\vartheta}, \tag{15}$$

$$\begin{aligned} \tilde{\vartheta} = {} & \frac{-q_0 h \sin^2 \vartheta(i)}{i} - \frac{K_3 \sin^3 \vartheta(i) \cos \vartheta(i)}{K_2 i^2} - \frac{\sin 4\vartheta(i)}{8i^2} \\ & + \frac{\vartheta(i+1) + \vartheta(i-1)}{2} + \frac{\vartheta(i+1) - \vartheta(i-1)}{4i}, \end{aligned} \tag{16}$$

for $i \in \{1, \ldots, n-1\}$ (bulk). As usual, $h = 1/n$ and $\hat{r} = ih$. In the calculations, $n = 100$ was used. The over-relaxation factor ω was chosen as 1.8.

In the case of planar-free boundary coupling, the value of ϑ at the boundary is not prescribed but, rather, has to be determined such as to satisfy Eq. (12) ($i = n$ corresponds to $\hat{r} = 1$):

$$\begin{aligned} \vartheta^{new}(n) = {} & q_0 h - \frac{h \sin 2\vartheta(n)}{2} + \frac{K_{24} h \sin 2\vartheta(n)}{2K_2} \\ & + \vartheta(n-1). \end{aligned} \tag{17}$$

The problem turned out to be ill-conditioned, so that double precision was necessary. Using $n = 100$, the maximum difference between the solution on the grid and the analytical solution Eq. (14) was less than 5×10^{-6}.

III. RESULTS

A. Fixed boundary conditions

Experimentally, rigid anchoring at the capillary wall in the direction of the capillary axis can be accomplished

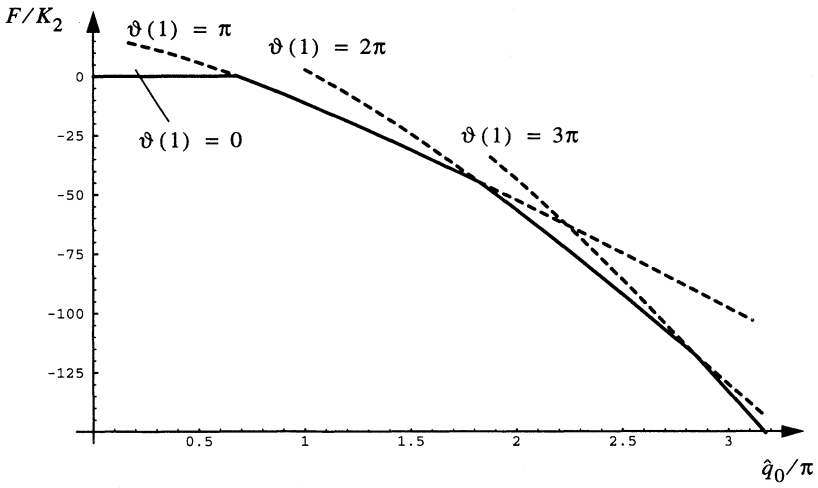

FIG. 2. Energies of the equilibrium director configurations as a function of the (dimensionless) twisting power $\hat{q}_0$ for cases where the director between the center and the capillary wall rotates by $m\pi$, $m = 0 \cdots 3$. The lowest energies are plotted as a solid line, whereas the energies of the metastable states are shown as dotted lines.

by photopolymerization [12]. In order to find out which director configurations are stable, we have analyzed the director configurations for various values of the (dimensionless) twisting power d_{cap}/p_0, where d_{cap} is the capillary diameter, and for cases where the director field between the center and the wall of the capillary rotates by $m\pi$, m being $0, 1, 2, 3$. The computations have been performed for $K_3 = 2K_2$, which is quite realistic for most thermotropic mixtures; actually, the value of K_3 turned out to be of minor influence here. K_{24} was not needed here due to the fixed boundary conditions, so we chose it to be zero. We do not present the solutions $\vartheta(\hat{r})$, because they are not very elucidating, in contrast to the corresponding energies, which are presented in Fig. 2. The crossover points, expressed by the values of d_{cap}/p_0, are (1) $d_{0\leftrightarrow 1} = 0.68$, (2) $d_{1\leftrightarrow 2} = 1.83$, and (3) $d_{2\leftrightarrow 3} = 2.84$, where the subscripts indicate the corresponding values of m.

They mark the stability range of the respective director configurations characterized by a rotation of $m\pi$ between the center and the wall. For example, the configurations where the director field rotates by π, should be stable for $d_{cap}/p_0 \in \{0.68, 1.83\}$, etc.

B. Planar-free boundary coupling

Planar-free boundary coupling occurs at untreated glass surfaces. Clearly, this is the more relevant part of this contribution, because the experimental technique of generating a preferred direction inside a capillary is very new.

We have computed the equilibrium configurations for $K_2 = K_{24} = K_3/2$, and for various values of $\hat{q}_0$. As a result, it turns out that the overall rotation angle between the center and the capillary wall does not increase continuously with increasing $\hat{q}_0$ but, rather, as a series of steps. See Fig. 3.

Qualitatively, these steps can be understood as the consequence of the director field trying to minimize the saddle-splay energy (per unit length), which is minimal if $\mathbf{n}$ is perpendicular to the capillary axis, and maximal if $\mathbf{n}$ is parallel; cf. Eq. (9). The latter position is obviously avoided.

We have also varied K_3 in order to analyze its influence on the director configuration. From Eq. (6) it can be deduced that the bend energy also induces the tendency to avoid the director position parallel to the capillary axis,

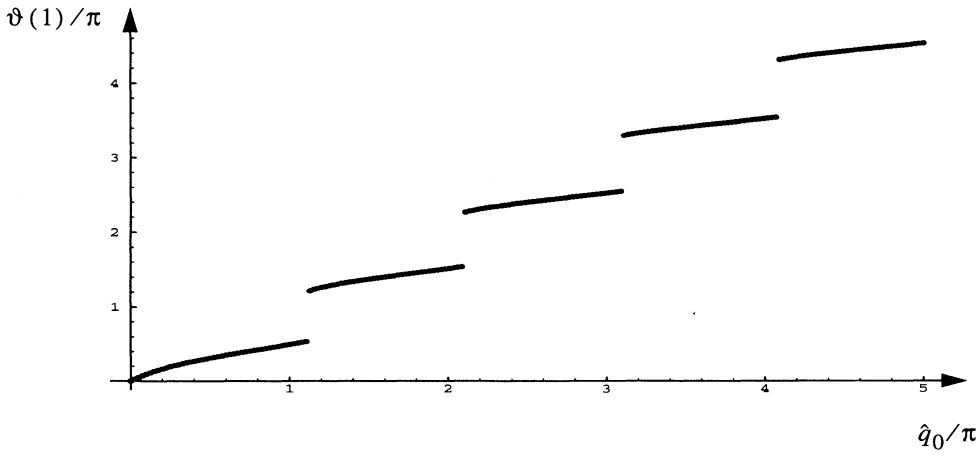

FIG. 3. Overall rotation $\vartheta(1)/\pi$ of the director between the center and the wall for 200 equidistant values of $\hat{q}_0/\pi = (q_0 r_{cap})/\pi = d_{cap}/p_0$. The steps occurring are the consequence of a preferred director orientation at the surface which is induced by the K_{24} term.

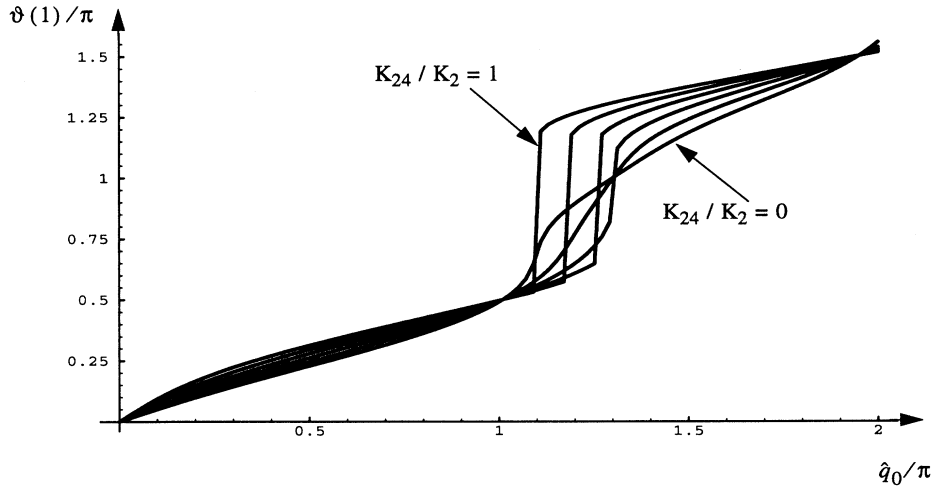

FIG. 4. Same as Fig. 3, but for various values of the saddle-splay constant and a smaller range of d_{cap}/p_0. In particular, $K_{24}/K_2 = \{0, 0.2, 0.4, 0.6, 0.8, 1\}$.

not only at the boundary, but everywhere in the bulk. We found that there is not much difference between $K_2 = K_3$ (one-constant approximation) and $K_3 = 2K_2$ (realistic value). We have also checked that the discontinuous behavior does not vanish even if $K_3 = 0$. So it became clear that the steps in Fig. 3 are a consequence of the saddle-splay energy. Since so far K_{24} could have been measured only by using submicrometer-sized geometries, this result may be interesting for experimentalists because it is valid for arbitrary capillary diameters and therefore allows for a convenient choice of the capillary size.

In order to relate our computations to future experiments, we present again the overall rotation as a function of $\hat{q}_0/\pi$, but look now only at one step, considering various values of K_{24}/K_2. From the step height and shape, K_{24} may be deduced. See Fig. 4.

IV. CONCLUSIONS

Some director configurations of a cholesteric compound confined to a capillary with planar orienting surface have been calculated employing the assumption that the director field is (1) rotationally symmetric, and (2) homogeneous along the capillary axis.

We are aware that this is usually not the case. More specifically, experimental results [12] revealed that for the setup discussed in Sec. III A, the director configuration occurring when $p_0 \approx d_{cap}$ is topologically equivalent (smoothly transformable) to the ansatz Eq. (5) with $\vartheta(1) = \pi$. The difference is that the location where the director is parallel to the capillary axis is slightly eccentric, and it spirals around the capillary axis. We trust that the result of Sec. III A, which predicts stability if $d_{cap}/p_0 \in \{0.68, 1.83\}$, is generally valid, since this symmetry-breaking three-dimensional (3D) configuration is quite similar to the 1D ansatz used here. The configurations with $\vartheta(1) > \pi$, however, might not be ground states but, rather, director fields with the usual cholesteric defects are preferred.

In Sec. III B, planar-free boundary conditions have been examined. One interesting feature of the geometry studied is that the saddle-splay energy Eq. (9) acts equivalently to a Rapini surface energy

$$f_{Rapini} = \frac{W}{2}\sin^2(\vartheta - \vartheta_{easy}),$$

$$\text{with} \quad W = \frac{K_{24}}{r_{cap}} \quad \text{and} \quad \vartheta_{easy} = \frac{\pi}{2}. \quad (18)$$

As a consequence, "forbidden directions" for the surface orientations are induced. We prefer to speak of forbidden directions rather than of easy axes because in our calculations, these forbidden directions are avoided by a discontinuous overall rotation of the director as a function of d_{cap}/p_0. The step height of the overall rotation is related to K_{24}/K_{22} and, therefore, this effect should provide a method by which to determine the saddle-splay constant in conveniently sized capillaries. This should be possible because the pitch of a given material can be made arbitrarily large by varying the concentration ratio of the enantiomers.

Again, for materials with short pitch, quite different configurations might be energetically preferred, so that the function presented in Fig. 3 is probably invalid above a certain value of d_{cap}/p_0.

ACKNOWLEDGMENTS

We thank Dr. Heinz Kitzerow for valuable discussions. The financial support of the Deutsche Forschungsgemeinschaft via the Sonderforschungsbereich "Anisotrope Fluide" is gratefully acknowledged.

[1] J. Nehring and A. Saupe, J. Chem. Phys. **56**, 337 (1971).
[2] D. W. Allender, G. P. Crawford, and J. W. Doane, Phys. Rev. Lett. **67**, 1442 (1991).
[3] S. Kralj and S. Žumer, Phys. Rev. A **45**, 2461 (1992).
[4] S. Žumer and S. Kralj, Liq. Cryst. **12**, 613 (1992).
[5] R. D. Polak *et al.*, Phys. Rev. E **49**, 978 (1994).
[6] R. J. Ondris-Crawford *et al.*, Phys. Rev. E **48**, 1998 (1993).
[7] A. Kilian, Liq. Cryst. **14**, 1189 (1993).
[8] G. Barbero, A. Sparavigna, and A. Strigazzi, Nuovo Cimento D **12**, 1259 (1990).
[9] S. Meiboom, J. P. Sethna, P. W. Anderson, and W. F. Brinkman, Phys. Rev. Lett. **46**, 1216 (1981).
[10] P. G. De Gennes and J. Prost, *The Physics of Liquid Crystals*, 2nd ed. (Clarendon Press, Oxford, 1993).
[11] E. M. Terent'ev and S. A. Pikin, Sov. Phys. Crystallogr. **30**, 131 (1985).
[12] H. Kitzerow (private communication).